Diffusion-Controlled Semibatch Emulsion Polymerization of Styrene

C. S. CHERN

Department of Chemical Engineering, National Taiwan Institute of Technology, Taipei, Taiwan, Republic of China

SYNOPSIS

Semibatch emulsion polymerization of styrene under the monomer-starved condition is strongly affected by the gel effect. A mechanistic model based on diffusion-controlled reaction mechanisms is developed to predict the kinetics of semibatch emulsion polymerization. Experimental data available in the literature are employed to assess the proposed model. Reasonable agreement between the model predictions and experimental data is observed. The simulation results suggest that the reaction system approaches Smith–Ewart case II kinetics ($\bar{n} = 0.5$) when the concentration of monomer in the particles is close to the saturation value, whereas the reaction system under the monomer-starved condition is characterized by diffusion-limited reaction mechanisms ($\bar{n} \gg 0.5$). © 1995 John Wiley & Sons, Inc.

INTRODUCTION

Emulsion polymerization is a process in which most of the propagation reaction takes place in the segregated particles (50–1000 nm in diameter) dispersed in water. These innumerable particles can be stabilized by anionic surfactants which impart repulsive forces between similarly charged electric double layers to the emulsion polymer. Semibatch emulsion polymerization is an important process for commercial production of polymeric materials because of limitations of heat transfer in large-scale reactors. In a typical semibatch process, most of the water along with the initial surfactant and monomer is charged to the reactor. The initial reactor charge is then brought to the reaction temperature, followed by the addition of initiator solution to initiate the reaction. After a period of time, the remaining monomer is fed to the reactor over a few hours. The rate of monomer addition can be determined by the rate of polymerization (i.e., the rate of heat generation) and the cooling capacity of the reactor system. Polymerization temperature is kept constant throughout the reaction. After the end of monomer addition, the reactor temperature is maintained at the same level for about 1 h to reduce the residual monomer to an acceptable level. Nowadays latex products are widely used in coatings, adhesives, plastics, and rubber industries.

Wessling[1] analyzed the kinetics of semibatch emulsion polymerization and predicted that the reaction system which followed Smith–Ewart case II kinetics[2-4] would approach a pseudo-steady state if the rate of monomer addition R_a was kept constant. In the pseudo-steady state, the rate of polymerization R_p depends on R_a according to the following equation:

$$1/R_p = 1/K + 1/R_a \tag{1}$$

where $K = K_p N_p \bar{n}/(N_a V_m)$. Here, K_p is the propagation rate constant, N_p is the number of particles per cubic centimeter of latex, $\bar{n}$ is the average number of free radicals per particle, N_a is Avogadro's number, and V_m is the molar volume of monomer. Recently Dimitratos[5] reached the same conclusions using a more rigorous treatment and his derivation showed that Eq. (1) was also valid for more water-soluble monomers such as vinyl acetate and methyl acrylate.

The pseudo-steady-state behavior predicted by eq. (1) was tested against Gerrens' data on a water-insoluble monomer styrene,[6,7] which was assumed to obey Smith–Ewart case II kinetics (i.e., $\bar{n} = 0.5$). Gerrens presented two sets of R_p-vs.-R_a data. In the

Journal of Applied Polymer Science, Vol. 56, 221–230 (1995)
 CCC 0021-8995/95/020221-10

first series of experiments, all of the water, surfactant, and initiator and 17.1% of the total monomer were charged to the reactor to start the reaction. Nucleation of primary particles took place at 50°C over 30 min. The remaining monomer was then added to the reactor at a prescribed feed rate. Polymerization temperature was kept at 50°C throughout the reaction.

In the second series using the monomer emulsion feed technique, the reaction started in the part of the whole recipe initially charged to the reactor. Contrary to the runs with the monomer feed, the monomer emulsion feed brought more and more surfactant/water into the reaction medium. The primary function of the surfactant in the monomer emulsion feed is to stabilize the growing particles. Nevertheless, feeding surfactant to the reaction vessel might cause secondary nucleation and affect the reaction kinetics through N_p present in the parameter K [see Eq. (1)]. Furthermore, addition of water, associated with the monomer emulsion feed, to the reactor will lead to dilution of both particles (reaction loci) and initiator. Change in the concentration of particles or initiator in water might cause the reaction system to deviate from Smith–Ewart case II kinetics.

The concise model of Wessling failed to predict the R_p-vs.-R_a data for the monomer feed process.[1] The calculated R_p was lower than the experimental data in the range of R_a investigated. Deviation from the pseudo-steady-state behavior is most likely caused by the assumption of Smith–Ewart case II kinetics. Reasonable agreement between the theory and experimental data was achieved for the monomer emulsion feed process. However, the success of the model in the series with the monomer emulsion feed should be accepted with reservations due to the above-mentioned complexity added to the reaction kinetics.

The primary locus of reaction in emulsion polymerization is generally believed to be inside the particle in which the concentration of polymer is so high that the viscosity of the reaction medium is very high. This is especially true for semibatch emulsion polymerization under the monomer-starved condition. Thus, extensive chain entanglements and low free volume greatly reduce the translational and segmental mobility of polymeric radicals. The termination reaction becomes diffusion controlled. This will result in a buildup in radicals and, consequently, increase the rate of polymerization if desorption of radicals from particles is negligible. This so-called gel effect in batch emulsion polymerization of styrene has been studied by several researchers.[8–10] It is postulated that it is the gel effect that is responsible for the discrepancy displayed by the Wessling model. The objective of this work was to develop a model based on diffusion-controlled reaction mechanisms to describe the kinetics of semibatch emulsion polymerization of styrene.

MODEL DEVELOPMENT

The rate of polymerization for semibatch emulsion polymerization can be written as

$$R_p = K_p[\mathrm{M}]_p(\bar{n}N_p/N_a) \tag{2}$$

where $[\mathrm{M}]_p$ is the concentration of monomer in the particles, which shows an upper limit governed by an equilibrium between swelling pressure and interfacial tension.[11] The saturation concentration of styrene in the particles is 5.2×10^{-3} mol/cm^3, representing 46% conversion.[12] The $[\mathrm{M}]_p$ data as a function of percentage of monomer added are available in Ref. 7. Note that the reported values of R_p are normalized by dividing by the final latex volume, 2000 cm^3 (units of R_p : mol/cm^3 − s).[1,6,7]

The most difficult kinetic parameters in Eq. (2) to predict are N_p and $\bar{n}$. Here, N_p is determined by the process of particle nucleation, which is beyond the scope of this study. The value of N_p for the finished batch was determined to be 1.4×10^{15} cm^{-3} by electron microscopy.[7] Ugelstad and coworkers[13,14] derived the following equations to calculate $\bar{n}$ at steady state:

$$\alpha = \alpha' + m\bar{n} - Y\alpha^2 \tag{3}$$

$$\alpha = \rho_a V_p/K_{tp}N_p \tag{4}$$

$$\alpha' = \rho_i V_p/K_{tp}N_p \tag{5}$$

$$m = K_0 a_p/K_{tp} \tag{6}$$

$$Y = 2N_a K_{tw}K_{tp}/K_c^2 V_p N_p \tag{7}$$

where α, α', m, and Y are dimensionless groups related to absorption of radicals by particles, generation of radicals in water, desorption of radicals from particles, and termination in the aqueous phase, respectively. The term ρ_a is the rate of absorption of radicals by particles, ρ_i is the rate of production of radicals in water, V_p is the volume of a monomer-swollen particle, a_p is the surface area of a particle, K_{tp} is the termination rate constant in the particles, K_{tw} is the termination rate constant in the aqueous

phase, K_0 is the rate constant for desorption of radicals from particles, and K_c is the rate constant for capture of radicals by particles.

The desorption process involves transfer of the activity of polymeric radicals to monomer, emulsifier, and chain transfer agent, followed by diffusion of those monomeric radicals so produced to the aqueous phase.[15] Considering the relatively low values of water solubility of styryl radicals (assumed to be similar to that of styrene, ca. 0.03%)[16] and chain transfer to monomer constant (ca. 3×10^{-5} K_p to 6×10^{-5} K_p at 60°C),[17] desorption of radicals from particles is assumed to have an insignificant effect on the reaction kinetics. With the additional assumption that the termination reaction in water is not important, Eqs. (3)–(7) can be reduced to Stockmayer's solution:[18]

$$\bar{n} = a/4I_0(a)/I_1(a) \tag{8}$$

where $a = (8\alpha')^{1/2}$ and I_0 and I_1 are the Bessel functions of the first kind of order 0 and 1, respectively. Other assumptions used in the model development include the following:

1. The reaction is isothermal (50°C).
2. The inhibition reaction is not considered.
3. The rate of monomer addition is constant throughout the reaction.
4. The concentration of styrene in water is nil compared to that in the particles.
5. There is no secondary nucleation or coagulation of particles taking place during the monomer addition, that is, the total number of particles (reaction loci) available for polymerization is a constant.

In order to calculate $\bar{n}$ and hence R_p, the only task left is to determine $\alpha' = \rho_i V_p / K_{tp} N_p$ and K_p. Note that V_p will increase throughout the monomer addition period. The parameters ρ_i and V_p can be calculated as follows:

$$\rho_i = 2fK_{\text{dec}}[\text{I}]_w \tag{9}$$

$$V_p = W_m(\%\text{ monomer added})/\{N_p V_t[\rho_m(1 - \Phi_p) + \rho_p \Phi_p]\} \tag{10}$$

$$\Phi_p = 1 - ([\text{M}]_p \text{MW}_m/\rho_m) \tag{11}$$

where f is the initiator efficiency factor, K_{dec} is the initiator decomposition rate constant, $[\text{I}]_w$ is the concentration of initiator in the aqueous phase. In this work, $[\text{I}]_w$ can be regarded as a constant throughout the reaction because all water is charged to the reactor initially for the monomer feed process and the decomposition rate constant K_{dec} at 50°C (ca. 1.333×10^{-6} s^{-1})[19] is relatively low. Here, W_m is the total weight of monomer shown in the recipe, V_t is the total volume of the finished batch, ρ_m is the density of monomer, ρ_p is the density of polymer, Φ_p is the volume fraction of polymer in the particles, and MW_m is the molecular weight of monomer.

Since the viscosity of the growing particles is quite high under the monomer-starved condition, the translational movement of macroradicals is restricted. Thus, the termination reaction becomes diffusion controlled and the termination rate is greatly reduced. This will result in an increase in the concentration of free radicals in the particles and a corresponding increase in the rate of polymerization.

As the viscosity of the reaction mixture increases to a still higher level, the rate of polymerization remains fast but the termination component of the gel effect does not continue to change significantly. This limitation on the gel effect is attributed to residual termination. When the translational movement of growing polymer chains becomes seriously restricted, the rate of termination does not approach zero since the active chain ends still possess a certain degree of mobility due to the propagation reaction. Thus, the termination rate constant K_{tp} can be written as

$$K_{tp} = K_{t,t} + K_{t,p} \tag{12}$$

where $K_{t,t}$ is the translational termination rate constant and $K_{t,p}$ is the residual termination rate constant.

In general, $K_{t,t}$ has been correlated with conversion or free-volume parameters and takes the following form:[20–23]

$$K_{t,t} = K_{t,t0}\exp[B_t(1/V_{f0} - 1/V_f)] \tag{13}$$

where $K_{t,t0}$ is the termination rate constant at the reference fractional free volume V_{f0}, V_f is the fractional free volume of the polymer particles, and B_t is an adjustable parameter that is a measure of the degree of diffusion control.

By assuming additivity of the free volume of polymer and monomer, the fractional free volume of the reaction loci can be calculated by the following equations:[20]

$$V_f = V_{fm}(1 - \Phi_p) + V_{fp}\Phi_p \quad (14)$$

$$V_{fm} = 0.112 + 6.2 \times 10^{-4}T(°C) \quad (15)$$

$$V_{fp} = 0.0245 + 1.4 \times 10^{-4}[T(°C) - 82] \quad (16)$$

where V_{fp} and V_{fm} are the fractional free volumes contributed by polymer and monomer, respectively, and T is the polymerization temperature.

Gardon[24] first realized that the termination reaction could take place even when the movement of all chain segments was completely restricted. He proposed a lattice model which did not take into account the excess chain-end mobility provided by the propagation reaction. The following equation derived from the lattice model represents the theoretical lower limit of the termination rate constant:

$$(K_{tp}/K_p)_{\min} = 0.185(1 - \Phi_p)/\Phi_p \quad (17)$$

According to Soh and Sundberg,[20] the residual termination rate constant $K_{t,p}$ was related to the jump length and jump frequency (i.e., frequency of propagation). Thus, $K_{t,p}$ can be expressed as

$$K_{t,p} = f_t\pi(2j_c a_0^2/3)\ln\{1000[3/(2j_c a_0^2)^{3/2}/N_a[R^*]_p\pi^{3/2}\} \times a_0 N_a K_p[M]_p/(1000j_c^{1/2}) \quad (18)$$

$$j_c = X_{c0}/2\Phi_p \quad (19)$$

where f_t is the efficiency parameter, j_c is the entanglement spacing, a_0 is the average root-mean-square end-to-end distance per square root of the number of monomer units in the chain, X_{c0} is the minimum degree of polymerization for entanglement for pure polymer, and $[R^*]_p$ is the concentration of free radicals in the particles.

The fact that many vinyl polymer reactions do not proceed to complete conversion is a well-documented phenomenon. When the reaction temperature is lower than the glass transition temperature of polymer being formed, conversion does not reach 100%. When the movement of monomer in the particles becomes diffusion limited, the propagation reaction slows down and the rate of polymerization decreases rapidly. Eventually, the reaction ceases when the glass transition temperature of polymer–monomer mixture equals the reaction temperature. Arai and Saito[23] proposed a semiempirical equation for K_p to describe the limiting conversion phenomenon as shown below:

$$K_p/K_{p0} = D_m/D_{m0} = \exp\{B_p[1/(V_{f0})_m - 1/V_f]\} \quad \text{when } V_f < (V_{f0})_m \quad (20)$$

$$K_p = K_{p0} \quad \text{when } V_f > (V_{f0})_m \quad (21)$$

where K_{p0} and D_{m0} are the propagation rate constant and diffusion coefficient of monomer at zero conversion, respectively, D_m is the diffusion coefficient of monomer in the particles, B_p is an adjustable parameter, and $(V_{f0})_m$ is the critical fractional free volume at which the propagation rate constant starts to decline.

At this point, it is only necessary to assign values to the kinetic parameters in order to carry out the computer simulation with the proposed model. Experimental data available in the literature are used to assess the proposed diffusion-limited reaction mechanisms.

RESULTS AND DISCUSSION

Gerrens[6,7] used the monomer feed process to study the kinetics of semibatch emulsion polymerization of styrene at 50°C. The rate of monomer addition ranged from 1.43×10^{-7} to 1.37×10^{-6} mol/cm^3-s. The $\log(\bar{n})$-vs.-percent-monomer-added data for different values of R_a are shown as discrete points in Figure 1. The $\bar{n}$ data are obtained from the measured R_p and the calculated K_p using Eq. (2). The parameters necessary for computer simulations are obtained from the literature or estimated from the reaction conditions and are compiled in Table I.

The only remaining parameter that needs to be specified before computer modeling can be carried out is f_t, which determines the magnitude of $K_{t,p}$. Determination of $K_{t,p}$ and $\bar{n}$ involves a trial-and-error procedure shown below since the concentration of free radicals in the particles in Eq. (18) is unknown:

1. Assume a value for $\bar{n}$.
2. Compute $K_{t,p}$ according to Eqs. (18) and (19).
3. Compute K_{tp} according to Eqs. (12)–(16).
4. Compute $\bar{n}$ by means of Eqs. (8)–(11).
5. Compare the guessed and theoretical $\bar{n}$ values.
6. Go to step 1 until the guessed and theoretical $\bar{n}$ values are equal.

Figure 1(a) shows the model predictions (continuous curves) for various values of f_t. Also included

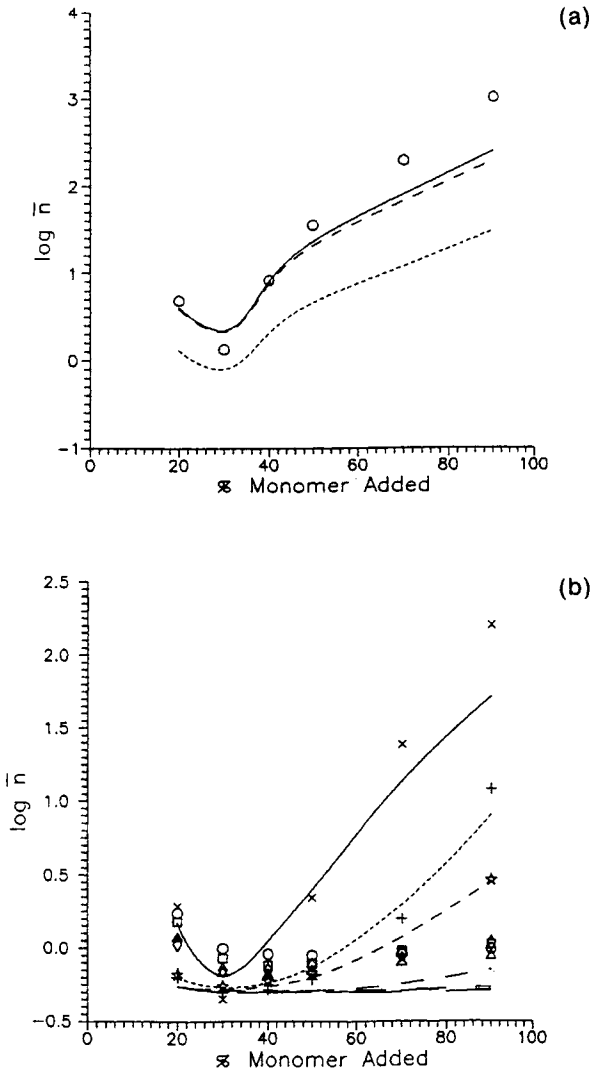

Figure 1 Average number of free radicals per particle as function of percent monomer added. (a) R_a = 1.43 $\times$ 10^{-7} mol/cm^3-s, (O) experimental data, (——) f_t = 0, (- - -) f_t = 0.01, (-----) f_t = 1; (b) (×, ——) R_a = 2.86 $\times$ 10^{-7}, (+, -----) R_a = 3.89 $\times$ 10^{-7}, (☆, - - -) R_a = 4.76 $\times$ 10^{-7}, (◇, — · —) R_a = 7.62 $\times$ 10^{-7}, (△, — - —) R_a = 9.53 $\times$ 10^{-7}, (□, — -- —) R_a = 1.14 $\times$ 10^{-6}, (O, — --- —) R_a = 1.37 $\times$ 10^{-6} mol/cm^3-s.

in Figure 1(a) are the log($\bar{n}$)-vs.-percent-monomer-added data (discrete points) for the run at a monomer feed rate of 1.43 $\times$ 10^{-7} mol/cm^3-s. This experiment with the slowest R_a is expected to show the strongest gel effect. The calculated $\bar{n}$ increases with a decrease in f_t and the model with f_t equal to zero gives the best fit of the experimental data. These results suggest that the residual termination reaction can be neglected. Thus, f_t will be set at zero hereafter. Please note that during the early stage of monomer addition $\bar{n}$ decreases to a minimum due to the accumulation of monomer in the particles (see the $[M]_p$-vs.-percent-monomer-added data shown in Fig. 3 of Ref. 7) and, subsequently, increases toward the end of polymerization, even under the pseudo-steady-state condition. Reasonable agreement between the model predictions and experimental data is observed.

Corresponding to Figure 1(a), the calculated K_{tp} and K_p as a function of percentage of monomer added for the run at a monomer feed rate of 1.43 $\times$ 10^{-7} mol/cm^3-s are shown in Figs. 2(a) and 3, respectively. The value of K_{tp} decreases with a decrease in f_t. In addition, the changes in K_{tp} during the monomer addition are more than three orders of magnitude when f_t < 0.01. The calculated log(K_p)-vs-percent-monomer-added data at a monomer feed rate of 1.43 $\times$ 10^{-7} mol/cm^3-s shown in Figure 3 indicate that the propagation reaction is diffusion controlled throughout the monomer addition. Similar to K_{tp}, K_p first goes up to a maximum very quickly and then declines as polymerization proceeds. Nevertheless, the changes in K_p during the monomer addition are only about two orders of magnitude because of the smaller value of B_p in Eq. (20).

It is interesting to compare the calculated K_{tp}/K_p with the lowest theoretical limits of K_{tp}/K_p developed by Gardon[24] for the run at a monomer feed rate of 1.43 $\times$ 10^{-7} mol/cm^3-s. The log(K_{tp}/K_p)-vs.-Φ_p data are illustrated in Figure 4, in which the solid line represents Gardon's predictions and the other three curves spanned over a narrow range of Φ_p (ca. 0.84–0.95) are the predicted results with various values of f_t by the present model. The range of Φ_p encoun-

Table I Kinetic Parameters for Semibatch Emulsion Polymerization of Styrene

Parameter	Numerical Value	Reference
MW_m	104 g/mol	
ρ_m	0.909 g/cm^3	25
ρ_p	1.05 g/cm^3	25
f	1	
K_{p0}	2.17 $\times$ 10^{10} exp[−3905/T (K)] cm^3/mol-s	26
K_{tp0}	1.8 $\times$ 10^9 cm^3/mol-s	10
B_t	0.6	10
B_p	0.38	10
V_{f0}[a]	0.1151	
$(V_{f0})_m$	0.047	10
X_{c0}	385	27
a_0	7.4 $\times$ 10^{-8} cm	27

[a] Value corresponds to 40% conversion.

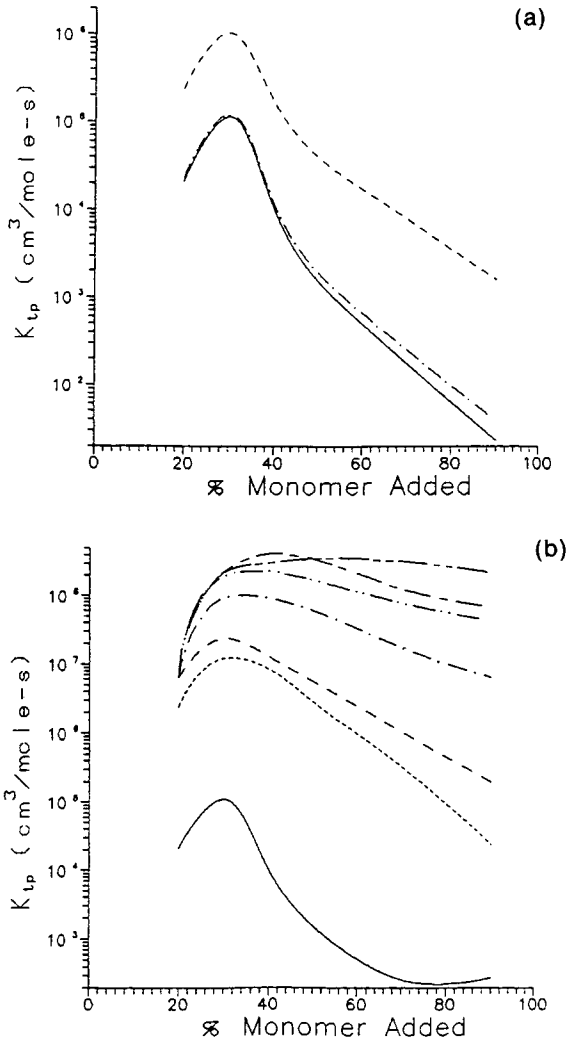

Figure 2 Termination rate constant as function of percent monomer added: (a) $R_a = 1.43 \times 10^{-7}$ mol/cm^3-s, (——) $f_t = 0$, (— · —) $f_t = 0.01$, (-----) $f_t = 1$; (b) (——) $R_a = 2.86 \times 10^{-7}$, (-----) $R_a = 3.89 \times 10^{-7}$, (- - -) $R_a = 4.76 \times 10^{-7}$, (— · —) $R_a = 7.62 \times 10^{-7}$, (— · · —) $R_a = 9.53 \times 10^{-7}$, (— - —) $R_a = 1.14 \times 10^{-6}$, (— -- —) $R_a = 1.37 \times 10^{-6}$ mol/cm^3-s.

tered in semibatch emulsion polymerization represents a monomer-starved condition and the log(K_{tp}/K_p)-vs.-Φ_p data support the proposed diffusion-controlled reaction mechanisms in this work. Figure 4 shows that the K_{tp}/K_p data with f_t equal to zero is approximately 10–100 times greater than the lowest theoretical limits when compared at a fixed Φ_p. The simulation results suggest that the segmental mobility and perhaps the translational movement of polymeric radicals play an important role in the termination reaction inside the relatively viscous particles.

The model with f_t equal to zero adequately pre-

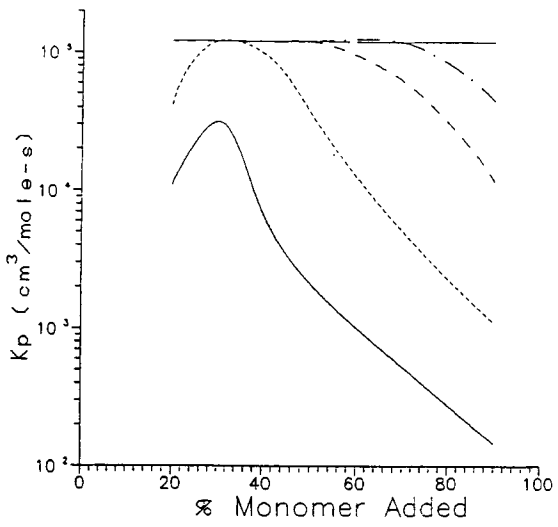

Figure 3 Propagation rate constant as function of percent monomer added: (——) $R_a = 1.43 \times 10^{-7}$, (-----) $R_a = 2.86 \times 10^{-7}$, (- - -) $R_a = 3.89 \times 10^{-7}$, (— · —) $R_a = 4.76 \times 10^{-7}$, (— · · —) $R_a = 7.62 \times 10^{-7}$, (— - —) $R_a = 9.53 \times 10^{-7}$, (— -- —) $R_a = 1.14 \times 10^{-6}$, (— --- —) $R_a = 1.37 \times 10^{-6}$ mol/cm^3-s.

dicts all of the features of log($\bar{n}$)-vs.-percent-monomer-added data for the entire range of R_a, as shown in Figure 1. The experimental data along with model predictions are also included in Table II for a closer examination, especially when $R_a > 7.62 \times 10^{-7}$ mol/cm^3-s. The results show that $\bar{n}$ decreases with an increase in R_a due to the lower viscosity and, consequently, faster termination reaction in the parti-

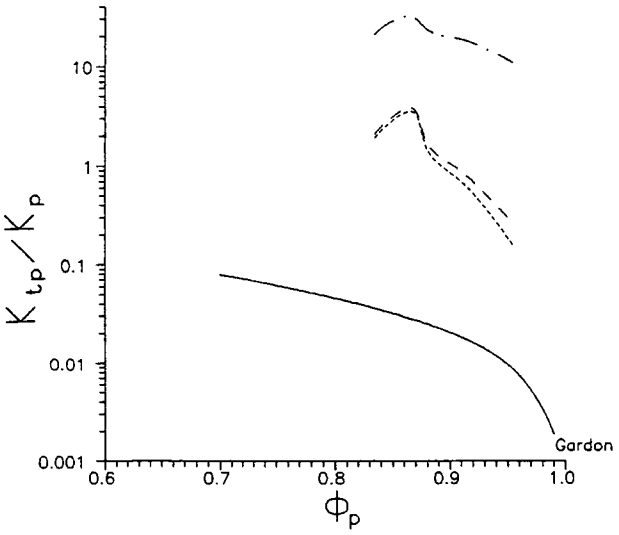

Figure 4 K_{tp}/K_p as function of volume fraction of polymer in particle: (——) Gardon, (-----) $f_t = 0$, (- - -) $f_t = 0.01$, (— · —) $f_t = 1$.

Table II $\bar{n}$-vs.-Percent Monomer Added and Model Predictions[a]

$R_a \times 10^7$ (mol/cm^3-s)	By Percent Monomer Added					
	20%	30%	40%	50%	70%	90%
1.43	4.86	1.35	8.32	35.8	200	1068
	(4.05)	(2.20)	(8.11)	(23.3)	(81.7)	(258)
2.86	1.92	0.45	0.66	2.19	24.5	161
	(1.49)	(0.65)	(1.11)	(2.48)	(13.7)	(52.3)
3.89	0.63	0.50	0.52	0.61	1.58	12.1
	(0.63)	(0.54)	(0.58)	(0.74)	(1.97)	(8.09)
4.76	0.67	0.55	0.60	0.68	0.86	2.90
	(0.55)	(0.52)	(0.55)	(0.63)	(1.18)	(2.85)
7.62	1.07	0.71	0.71	0.76	0.92	1.07
	(0.55)	(0.51)	(0.51)	(0.51)	(0.57)	(0.71)
9.53	1.19	0.69	0.67	0.71	0.81	0.89
	(0.55)	(0.50)	(0.50)	(0.51)	(0.52)	(0.54)
11.40	1.51	0.85	0.76	0.78	0.95	1.05
	(0.55)	(0.50)	(0.50)	(0.50)	(0.51)	(0.52)
13.70	1.72	0.99	0.91	0.89	0.90	0.98
	(0.55)	(0.50)	(0.50)	(0.50)	(0.50)	(0.51)

[a] Model predictions are given by numbers in parentheses.

cles. Moreover, Figure 1(b) shows that the runs with $R_a < 4.76 \times 10^{-7}$ mol/cm^3-s (monomer starved) are characterized by the diffusion-controlled reaction mechanisms. Whereas the runs with $R_a > 7.62 \times 10^{-7}$ mol/cm^3-s (near monomer saturated) approach Smith–Ewart case II kinetics.

Such a transition in the reaction kinetics is also evident in Figures 2 and 3. The predicted $\log(K_{tp})$-vs.-percent-monomer-added profiles are shown in Figure 2. When $R_a < 4.76 \times 10^{-7}$ mol/cm^3-s, K_{tp} decreases rapidly during the monomer addition period. As R_a continues to increase and ultimately approach the point in which the particles are saturated with monomer, the gel effect becomes less important. Figure 3 shows the calculated $\log(K_p)$-vs.-percent-monomer-added profiles. The curves with $R_a > 7.62 \times 10^{-7}$ mol/cm^3-s are rather flat, and they coincide with each other, which means that the propagation reaction is not diffusion limited. On the contrary, the runs with $R_a < 4.76 \times 10^{-7}$ mol/cm^3-s show a decrease in K_p as polymerization proceeds. The slower the rate of monomer addition, the stronger the effect of the diffusion process on the propagation reaction. Thus, it can be concluded that depending on R_a both diffusion-controlled reaction mechanisms and Smith–Ewart case II kinetics can be found in semibatch emulsion polymerization of styrene.

Table II shows that after 90% monomer was added to the reactor $\bar{n}$ has a value of 1068 for the run with $R_a = 1.43 \times 10^{-7}$ mol/cm^3-s. According to Eqs. (10) and (11), V_p is estimated to be 1.56×10^{-16} cm^3 and this $\bar{n}$ corresponds to a concentration of 1.14×10^{-5} mol/cm^3! For comparison, $[R^*]_p$ is only 5.35×10^{-9} mol/cm^3 if Smith–Ewart case II kinetics prevails. One may question whether such a high concentration of radicals within the tiny particles (ca. 6.67×10^{-6} cm in diameter) is practical. As mentioned above, the $\bar{n}$ data are obtained by means of Eq. (2), in which R_p, $[M]_p$, and N_p are available in the work of Gerrens and K_p is calculated according to Eqs. (14)–(16), (20), and (21). Apparently, it is the diffusion-controlled propagation ($K_p/K_{p0} = D_m/D_{m0} = 0.0012$) that is responsible for the very high $\bar{n}$. Note that the reported $[M]_p$ data only represent an average monomer concentration in the particles, based on the assumption that monomer is uniformly distributed in the particles. However, this might not be the case when considering the restricted diffusion of individual monomer molecules at low free volumes.

Chern and Poehlein[28] postulated that monomer molecules could freely move in the particles due to their relatively small size. Thus, monomer is most likely to be uniformly distributed within the particles. To support this concept, they then used the following equation to calculate the monomer concentration profiles in a particle:

$$[M]'_p = \sinh(\theta r')/[r' \sinh(\theta)] \qquad (22)$$

where $[M]'_p = [M]_{pr}/[M]_{ps}$, $r' = r/r_s$, and $\theta = r_s(K_p[R^*]_p/D_m)^{1/2} = r_s(K_{p0}[R^*]_p/D_{m0})^{1/2}$ [see Eq.

(20)]. Here, r is the radial distance from the center of the particle, r_s is the radius of the particle, and $[M]_{pr}$ and $[M]_{ps}$ are the monomer concentrations at r and r_s, respectively.

As shown in Figure 5, the monomer concentration gradient in the particle increases with increasing θ. For a very small value of θ (i.e., $\theta < 0.5$), no appreciable monomer concentration gradient is observed. For styrene, D_{m0} is estimated to be 2×10^{-6} cm^2/s at 60°C.[29] If D_{m0} is proportional to the absolute temperature according to the hydrodynamical theory or Eyring rate theory,[30] the value of $\bar{n}$ must be greater than 1.34×10^8 in order to have a value of θ greater than 1, that is, a nonuniform distribution of monomer in the particles. Thus, the simulation results based on Eq. (22) do not support a monomer concentration gradient in the particles at the point where $R_a = 1.43 \times 10^{-7}$ mol/cm^3-s and 90% monomer has been added to the reactor.

In an attempt to reconcile the different viewpoints, a core/shell model is proposed as follows. Considering the fact that (i) monomer must diffuse into the particles from the aqueous phase to compensate for consumption of monomer by propagation and (ii) the viscosity of the reaction medium is extremely high under the monomer-starved condition, the polymerizing particle is modeled as a heterogeneous system comprising a pure polymer core and a monomer-swollen shell as illustrated in Figure 6(b). For simplicity, monomer is assumed to be uniformly distributed in the shell phase. In this manner, the volume fraction of polymer in the core (Φ_{pc}) equals 1 and the volume fraction of polymer in the shell (Φ_{ps}) ranges from zero to 0.954. The greater the Φ_{ps}, the smaller the resistance for monomer molecules to penetrate the particles. For comparison, two limiting cases are also included in this diagram: (a) uniform distribution of monomer throughout the particles, that is, the resistance for monomer molecules to penetrate the particles is zero, and (c) a pure polymer core and a pure monomer shell, that is, the resistance for monomer molecules to penetrate the particles is infinite. In addition, the polymeric radicals are presumably located in the shell phase because a hydrophilic sulfate end group is attached to the incoming radical.

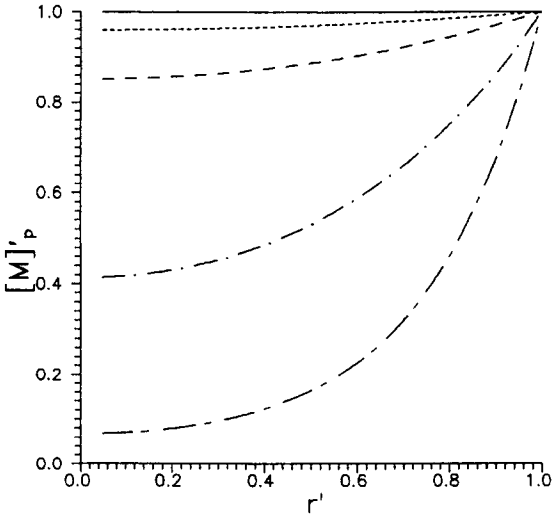

Figure 5 Dimensionless monomer concentration profiles as function of dimensionless radial distance from center of particle: (——) $\theta = 0.1$, (- - - -) $\theta = 0.5$, (– – –) $\theta = 1.0$, (— · —) $\theta = 2.5$, (— · · —) $\theta = 5.0$.

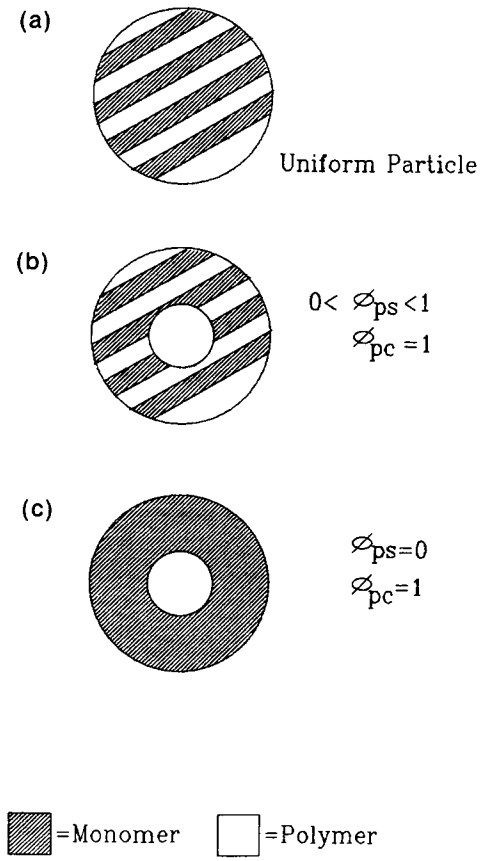

Figure 6 Core/shell model: (a) uniform particle, (b) pure polymer core and monomer-swollen shell, (c) pure polymer core and pure monomer shell.

The following equation is employed to compute the experimental $\bar{n}$:

$$R_p = K_p[M]_s(\bar{n}N_p/N_a) \tag{23}$$

where $[M]_s$ is the concentration of monomer in the shell. The theoretical $\bar{n}$ can be calculated by using

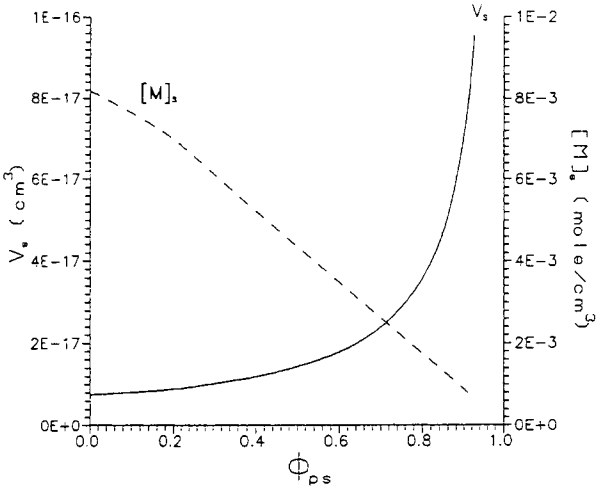

Figure 7 Volume of shell or concentration of monomer in shell as function of volume fraction of polymer in shell: (——) V_s, (- - - - -) $[M]_s$.

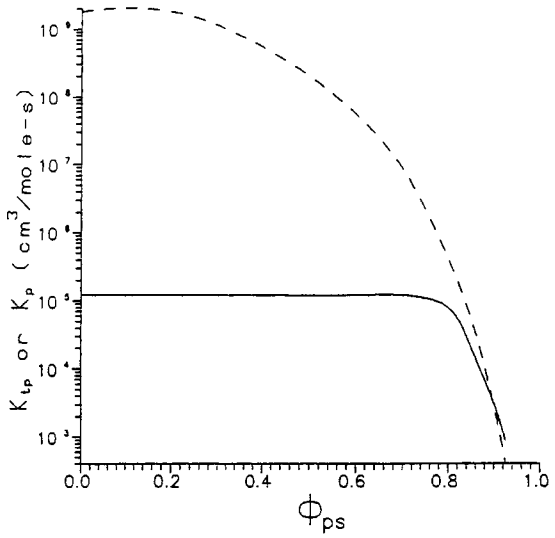

Figure 8 Termination rate constant or propagation rate constant as function of volume fraction of polymer in shell: (——) K_p, (- - - - -) K_{tp}.

Eqs. (8)–(10), (13), (15), and (16) in combination with the following equations:

$$V_f = V_{fm}(1 - \Phi_{ps}) + V_{fp}\Phi_{ps} \tag{24}$$

$$\Phi_{ps} = 1 - ([\mathrm{M}]_s \mathrm{MW}_m/\rho_m) \tag{25}$$

$$[\mathrm{M}]_s = \rho_m(1 - \Phi_{ps})/\mathrm{MW}_m \tag{26}$$

$$\alpha' = \rho_i V_s/N_p K_t \tag{27}$$

$$V_s = V_{s0}/(1 - \Phi_{ps}) \tag{28}$$

where V_s and V_{s0} are the volumes of the shell phase shown in Figures 6(b) and (c), respectively.

Figure 7 shows the calculated V_s and $[\mathrm{M}]_s$ versus Φ_{ps} curves for the point in which $R_a = 1.43 \times 10^{-7}$ mol/cm^3-s and 90% monomer has been added to the reactor. The extent of monomer penetration increases with an increase in Φ_{ps}. Consequently, V_s increases and $[\mathrm{M}]_s$ decreases with an increase in Φ_{ps}. The $\log(K_{tp})$ and $\log(K_p)$ vs. Φ_{ps} curves are shown in Figure 8. Here, K_{tp} decreases with an increase in Φ_{ps}, whereas K_p remains relatively constant before Φ_{ps} reaches a value of about 0.75 and then drops rather rapidly thereafter.

Figure 9 shows both the experimental data (discrete points) and theoretical values of $\bar{n}$ (continuous curve) predicted by the core/shell model as a function of Φ_{ps}. The intersection between the experimental data and model predictions occurs at the point where $\Phi_{ps} = 0.87$ and the corresponding $\bar{n} = 5.3$. Thus, $[\mathrm{R}^*]_p = \bar{n}/V_s N_a$ is calculated to be 1.6×10^{-7} mol/cm^3. Note that this value of $[R^*]_p$ derived from the core/shell model is 30 times greater than that of Smith–Ewart case II kinetics and it is about two orders of magnitude lower than that predicted by the model based on diffusion-controlled reaction mechanisms only. The simulation results suggest that the resistance for monomer molecules to penetrate the particles might not be that great, but the propagation reaction and hence the value of $\bar{n}$ [see Eq. (23)] is very sensitive to the extent of monomer penetration under the monomer-starved condition. Thus, such a core/shell model developed for distribution of monomer in the particles might be useful

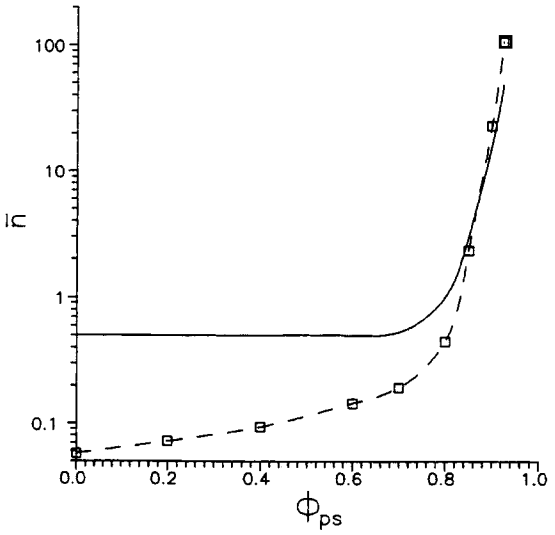

Figure 9 Average number of free radicals per particle as function of volume fraction of polymer in shell: (□, - - - - -) experimental data, (——) model predictions.

in describing the reaction kinetics of semibatch emulsion polymerization of styrene at extremely low free volumes.

CONCLUSIONS

A mechanistic model based on diffusion-controlled reaction mechanisms has been developed to predict the kinetics of semibatch emulsion polymerization of styrene. The termination reaction is governed by the translational diffusion-controlled mechanism. When the reaction medium becomes extremely viscous, even the monomer molecules do not readily diffuse in the particles. The propagation rate starts to decrease significantly, and this phenomenon plays an important role in the reaction kinetics of semibatch emulsion polymerization of styrene. The proposed model has been tested with experimental data available in the literature. The model adequately predicts all of the features of $\log(\bar{n})$-vs.-percent-monomer-added data for the entire range of monomer feed rate. The simulation results suggest that the reaction system approaches Smith–Ewart case II kinetics when the concentration of monomer in the particles is close to the saturation value, whereas the system is characterized by diffusion-controlled reaction mechanisms under the monomer-starved condition. For the run with a monomer feed rate of 1.43×10^{-7} mol/cm^3-s, the predicted concentration of free radicals in the particles is unusually high. In this regard, a core/shell model, in which the polymerizing particle is treated as a heterogeneous system comprising a pure polymer core and a monomer-swollen shell, is developed to predict the reaction kinetics of semibatch emulsion polymerization of styrene at extremely low free volumes.

REFERENCES

1. R. A. Wessling, *J. Appl. Polym. Sci.*, **12,** 309 (1968).
2. W. V. Smith and R. W. Ewart, *J. Chem. Phys.*, **16,** 592 (1948).
3. W. V. Smith, *J. Am. Chem. Soc.*, **70,** 3695 (1948).
4. W. V. Smith, *J. Am. Chem. Soc.*, **71,** 4077 (1949).
5. Y. N. Dimitratos, Ph.D. Dissertation, Chemical Engineering Department, Lehigh University, Bethlehem, PA, 1989.
6. H. Gerrens, paper presented to Polymer Division, American Chemical Society, Fall Meeting, 1966; *Polym. Prepr.*, **7**(2), 699 (1966).
7. H. Gerrens, *J. Polym. Sci.*, Part C, **27,** 77 (1969).
8. D. R. James and D. C. Sundberg, *J. Polym. Sci., Polym. Chem. Ed.*, **18,** 903 (1980).
9. B. Harris, A. E. Hamielec, and L. Marten, in *Emulsion Polymers and Emulsion Polymerization,* D. R. Bassett and A. E. Hamielec, Eds., ACS Symposium Series 165, American Chemical Society, Washington, DC, 1981, pp. 315–326.
10. D. C. Sundberg, J. Y. Hsieh, S. K. Soh, and R. F. Baldus, in *Emulsion Polymers and Emulsion Polymerization,* D. R. Bassett and A. E. Hamielec, Eds., ACS Symposium Series 165, American Chemical Society, Washington, DC, 1981.
11. M. Morton, S. Kaizerman, and M. W. Altier, *J. Coll. Sci.*, **9,** 300 (1954).
12. E. Bartholome, H. Gerrens, R. Herbeck, and H. M. Weitz, *Z. Elektrochem.*, **60,** 334 (1956).
13. J. Ugelstad, P. C. Mork, and J. O. Aasen, *J. Polym. Sci., A-1,* **5,** 2281 (1967).
14. J. Ugelstad and P. C. Mork, *Br. Polym. J.*, **2,** 31 (1970).
15. M. Nomura, M. Harada, W. Eguchi, and S. Nagata, in *Emulsion Polymerization,* I. Piirma and J. L. Gardon, Eds., ACS Symposium Series 24, American Chemical Society, Washington, DC, 1976.
16. F. V. Loncar, Jr., Ph.D. Dissertation in Polymer Science and Engineering, Lehigh University, Bethlehem, PA, 1985.
17. J. G. Braks and R. Y. M. Huang, *J. Appl. Polym. Sci.*, **22,** 3111 (1978).
18. W. H. Stockmayer, *J. Polym. Sci.*, **24,** 313 (1957).
19. I. M. Kolthoff and I. K. Miller, *J. Am. Chem. Soc.*, **73,** 3055 (1951).
20. S. K. Soh and D. C. Sundberg, *J. Polym. Sci., Polym. Chem. Ed.*, **20,** 1299, 1315, 1331, 1345 (1982).
21. K. Ito, *J. Polym. Sci., A-1,* **7,** 3387 (1969); **8,** 1313 (1970); **10,** 1481 (1972).
22. N. Friis and A. E. Hamielec, in *Emulsion Polymerization,* I. Piirma and J. L. Gardon, Eds., ACS Symposium Series 24, American Chemical Society, Washington, DC, 1976.
23. K. Arai and S. Saito, *J. Chem. Eng. Jpn.*, **9,** 302 (1976).
24. J. L. Gardon, *J. Polym. Sci., Part A-1,* **6,** 2851 (1968).
25. H. F. Mark, N. G. Gaylord, and N. Bikales, Eds., *Encyclopedia of Polymer Science and Technology,* Interscience, New York, 1964.
26. M. S. Matheson et al., *J. Am. Chem. Soc.*, **71,** 497 (1949).
27. J. D. Ferry, *Viscoelastic Properties of Polymers,* 2nd ed., Wiley-Interscience, New York, 1970.
28. C. S. Chern and G. W. Poehlein, *J. Polym. Sci., Polym. Chem. Ed.*, **25,** 617 (1987).
29. H. C. Lee, Ph.D. Dissertation, Chemical Engineering Department, Georgia Institute of Technology, Atlanta, GA, 1985.
30. R. B. Bird, W. E. Stewart, and E. N. Lightfoot, *Transport Phenomena,* Wiley, New York, 1960.

Received August 1, 1994
Accepted August 26, 1994